Journal Of Integrated Engineering And Management Sciences
ISSN: **3139-5511,** Volume-1 Issue-2, April-June 2026 | **JIEMS-1201**
DOI: https://doi.org/10.5281/zenodo.22333025

PROTOTYPICAL SIMULATION OF AN OPTICAL EDGE FILTERDESIGN FOR THREE DIFFERENT RAYLEIGH WAVELENGTHS USING OCTAVE SOFTWARE

***DR. T.SRINIVAS,** *Professor in Dept of ECE & Principal,*
MOTHER THERESSA COLLEGE OF ENGINEERING & TECHNOLOGY, PEDDAPALLI.

ABSTRACT: Over the past few decades, researchers have worked hard to create optical filters that let some wavelengths through but block others. Multi-coated optical screens are becoming more popular. Layer thickness changes the functionality of these filters, giving them several uses. Quarter wave stack (QWS) technique makes edge filters and other optical filters. Optimization is needed to meet minimal standards. The QWS model and Octave's optical matrix technique will be used to create an optical edge filter. The design used Si and MoS2, both low- and high-refractive-index materials. The results show 24 layers is best. Increased transmittance allows this. The design modeling employed "glass|12HL|air." for the 405 nm, 532 nm, and 633 nm (ex) Rayleigh wavelengths. After building and testing the optical edge filter, Cuton and Cutoff values are found. Three cut-on frequencies are detected at 408.11, 536, and 640.25 nm. The three matching activities had MET values of 32.3%, 31.3%, and 32%. This research demonstrates that the predicted value and model differ by 0.2, 1.7, and 1.15 nm for the three ex values (405, 532, and 633 nm). While the estimated value is lower, the Cutoff figures are substantially higher. Some filters show 32% modulation transfer efficiency (MET) at the Rayleigh wavelength, whereas others show 32.3%, 31.3%, or 32%.
Keywords*: Optical filter; cut-on wavelength; minimum effective transmission.*

1. INTRODUCTION

Analytical instruments, clinical chemistry, fluorescence, microscopes, Raman spectrometers, and machine vision inspections have all contributed to optical filters' meteoric rise in popularity. At this time, the following are available: Band stop, low pass, high pass, and band pass filters are the four main categories of filters .

The manufacturing of optical filters makes use of two processes. The first method makes use of the deposited materials' natural capacity to absorb light within a narrow spectrum. An absorption filter is a type of filter that quickly degrades when heated. Light interference can also produce many different kinds of events. Due to the designer's considerable leeway, the filter design approach is well-suited for thin film filters. A multi-layer interference filter is made up of materials with different refractive indices. The thickness of any given material is proportional to a quarter of its wavelength. Variations in the number, thickness, and refractive index affect the quality of these optical filters .

The advantages of employing various materials are presented using MTF screens. Use of MTF filters is required for optimal results. All things considered, these improve the wave

ISSN: **3139-5511,** Volume-1 Issue-2, April-June 2026 | **JIEMS-1201**
DOI: https://doi.org/10.5281/zenodo.22333025

front's transmission, reflection, blocking, and general properties. Multiple interfaces exist in thin films, each subjected to compressive stresses from various materials. Among MTF's many uses are those of an optical filter, computer disk, anti-reflector, solar cell, and telecom component .

The MTF filter created from the quarter-wave stack (QWS) model is necessary for all optical filters. This filter comprises of numerous layers of dielectric materials with variable conductivities. QWS models are essential for thin-film screens composed of materials with diverse refractive indices. A quarter of an optical wavelength is sufficient to produce a powerful reflection of a single optical wavelength. The quarter wave stack is a versatile and uncomplicated method that can be applied to any material, making it more straightforward compared to alternative approaches .

MTF filter-based QWS models have been constructed utilizing several techniques such as spray pyrolysis, thermal evaporation, RF magnetron sputtering, and sol-gel. Modeling enables optical filters to achieve precise specifications for transmission accuracy, cut-on/cut-off wavelength, layer count, and thickness. This study constructs a modulation transfer function (MTF) filter utilizing the Octave programming language. The application distinguishes itself with its user-friendly interface, user-defined code extension, and built-in support for complex integers .

QUARTER-WAVE STACK

A vital component in the creation of thin film filters is the quarter-wave. According to M A Butt et al. (2017), the structure is defined by periodic layers with alternating thicknesses and refractive indices H and L. It is documented that band stop, short pass, and long pass filters are used.It is also used in the manufacturing of highly reflective laser mirror coatings..

2. EFFECT OF NUMBER OF LAYERS INDESIGN OPTICAL FILTER

Multi-layered optical thin-film structures use materials with different refractive indices. Layer hierarchy comes from lower (L) and higher (H) indices. From micrometers (m) to nanometers (nm), layers vary in thickness. In their 2019 work, Vaida, Birdeanu, and Birdeanu demonstrate the feasibility of stacked filters.

The setup: When dropped or broken, glass breaks into many tiny fragments due to its fragility.

Multilayer optical filters' transmission and reflection separation abilities depend on their layer count. More layers make changing reflectance or transmittance easy.

EQUATIONS FOR MULTILAYER THIN FILM (MTF) ASSEMBLY OPTICAL FILTER DESIGN

Use the following matrix to determine the optical properties of the underlying layers. Each layer generates mathematical matrices that impact magnetic and electric field qualities. The transmittance or reflectance coefficient is calculated by comparing substrate and impact medium admittances to the thin-film surface.

Journal Of Integrated Engineering And Management Sciences
ISSN: **3139-5511,** Volume-1 Issue-2, April-June 2026 | **JIEMS-1201**
DOI: https://doi.org/10.5281/zenodo.22333025

$$\begin{bmatrix} E \\ H \end{bmatrix} = M \begin{bmatrix} 1 \\ \eta_S \end{bmatrix} \quad (1)$$

It was decided to use vectors E and H, matrix M, as well as electric and magnetic fields.

$$\begin{bmatrix} E_a \\ H_a \end{bmatrix} = \begin{bmatrix} \cos\delta & i\sin\delta/\eta_1 \\ i\eta_1\sin\delta & \cos\delta \end{bmatrix} \begin{bmatrix} \cos\delta_2 & i\sin\delta_2/\eta_2 \\ i\eta_2\sin\delta_2 & \cos\delta_2 \end{bmatrix} \begin{bmatrix} 1 \\ \eta_3 \end{bmatrix} \quad (2)$$

$$M_r = \begin{bmatrix} 1 \\ \eta_S \end{bmatrix} \begin{bmatrix} cos\delta r & \frac{i}{\eta} sin\delta r \\ \eta i sin\delta r & cos\delta r \end{bmatrix} \quad (3)$$

$$M = M_L M_{L-1} \ldots .Mr \quad .M_2 M_1 r \quad \ldots M_2M_1 \quad (4)$$

The 2x2 Matrix M depicts the system's rth thin film. Since its beginning, the grid has remained unchanged.

$$\begin{bmatrix} B \\ C \end{bmatrix}$$

A "standard matrix assembly" is a series of procedures that are carried out from start to finish. The standardized electric field of the front contact can be calculated using the B(E) formula. The standardized magnetic field of the front contact is denoted by the symbol C(H). Before everything else,

$$(\delta i)\text{i})\text{f}$$

A layer wave is formed b

$$\delta r = \frac{2\pi}{\lambda} nidicos\phi \text{r=2π/λnidicosϕ}$$

$$\delta_r = \left(\frac{2\pi}{\lambda}\right) d_r (n_r^2 - k_r^2 - n_0^2 \cos^2 v_o - 2in_r k_r)^{1/2} \quad (5)$$

$$\eta_p = \frac{n}{cos\phi} \text{ for P- polarization} \quad (6)$$

$$\eta_S = ncos\phi \text{ for S- polarization} \quad (7)$$

And also

$$\rho = \left[\frac{\eta_{0-Y}}{\eta_{0+Y}}\right] \text{=η_o-Y/η_o+Y but } Y \text{ is admittance of multilayer thin film}$$

$$Y = \frac{B}{C} = \frac{\eta_{0\cos\delta} + \eta_1 \sin\delta}{\cos\delta + i\left(\eta_s/\eta_1\right)\sin\delta} \quad (8)$$

$$R = \rho\rho^* \text{ =ρρ^*ρρ^* } = \left[\frac{\eta_{0-Y}}{\eta_{0+Y}}\right] \left[\frac{\eta_{0-Y}}{\eta_{0+Y}}\right]^* \text{ the amplitude of the reflectance coefficient is representing by } \rho \quad (9)$$

$$T = \frac{4\eta_0 Re(Y)}{(\eta_{0+Y})(\eta_{0+Y})} \quad (10)$$

$$(\ cm^{-1}) = \frac{10^7}{\lambda ex(nm)} - \frac{10^7}{\lambda(nm)} \text{ 10^7/λex(nm)-10^7/λ(nm)} \quad (11)$$

3. RESULTS AND DISCUSSION

The simulation spans the wavelength range of 300-1000 nm and features three unique edge filters. These bands contain wavelengths of 405 nm, 532 nm, and 633 nm, respectively. As a result, three separate scenarios emerge, indicated as Case I, Case II, and Case III. When the transmission and reflectance are plotted against the wavelength, the number of layers remains constant. the one Raman devised

Case I: Edge Filter of Rayleigh Wavelength (λ_{ex})405 nm

Table 2 depicts the glass substrate layer architecture as well as the predicted Si and MoS2 thicknesses. The curves for reflectance and transmittance are shown in Figure

Journal Of Integrated Engineering And Management Sciences
ISSN: **3139-5511,** Volume-1 Issue-2, April-June 2026 | **JIEMS-1201**
DOI: https://doi.org/10.5281/zenodo.22333025

Table 1. Target Value of, λ_{cut-on} and $\lambda_{cut-off}$ correspond to different λ_{ex} for simulation

S/N	λ_{ex} (nm)	Target λ_{cut-on} (nm) corresponds to 200 cm^{-1} Raman shifts.	Target $\lambda_{cut-off}$ (nm) corresponds to 4000 cm^{-1} Raman shifts
1	405	408.31	483.29
2	532	537.70	675.81
3	633	641.10	847.67

Table 2. Calculated thickness of individual layer of MoS_2 and Si for filter correspond to λ_{ex} = 405 nm

Number of layers	Materials	Thickness (nm)
Air		
24	Si	32.64
23	MoS_2	21.54
2	Si	32.64
1	MoS_2	21.54
Substrate		

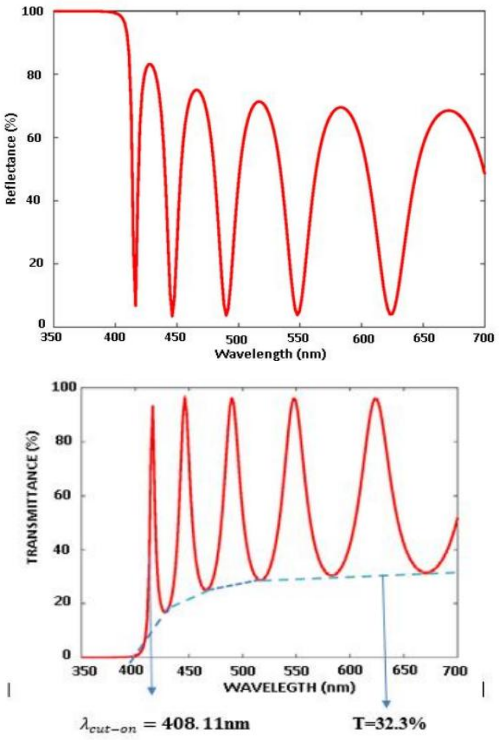
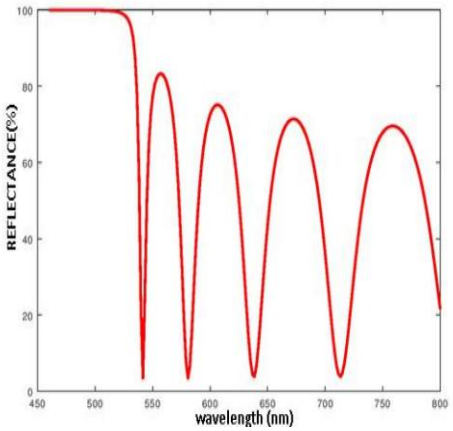


Fig. 1. Reflectance and transmittance against λfor λ_{ex} = 405 nm



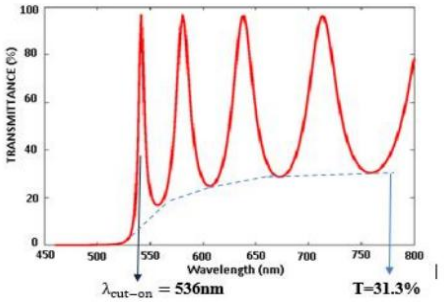


Fig. 2. Reflection and transmittance against λ for λ_{ex} = 532 nm

It is used in conjunction with the MTF edge filter. Even though it is terribly deformed, the reflection on the right side is fantastic.

$$\lambda_{cut-on} \text{ and } \lambda_{cut-off}$$

Readings at 408.11 nm and 700 nm wavelengths were possible. According to the data, the filter has a 33% mean efficiency of transfer (MET). 5.2

Case II: Edge Filter of Rayleigh Wavelength of 532nm

Table 3 shows the thickness of each layer in a glass-based system. Figure 2 depicts the relationship between transmittance and reflectance. The filter that distinguishes between separate elements within an image.

$$\lambda_{ex} = 532 \text{ nm},$$

$$\lambda_{cut-on} = 536 \text{ nm and } \lambda_{cut-off} = 800 \text{ nm}.$$

The results show that the filter has a 31.3% MET (Mean Efficiency Test)

Case III: Edge Filter of Rayleigh Wavelength of 633 nm

Table 4 shows the thickness of each layer using the same materials and number of layers as before. Figure 3. As a result, the edge filter of

λ_{ex} = 633 nm with λ_{cut-on}

$\lambda_{cut-off}$

It was discovered between 640.25 nm and 1000 nm. The filter's MET turns out to be 32%.

Journal Of Integrated Engineering And Management Sciences
ISSN: **3139-5511,** Volume-1 Issue-2, April-June 2026 | **JIEMS-1201**
DOI: https://doi.org/10.5281/zenodo.22333025

Table 3. Calculated thickness of individual layer of MoS_2 and Si for filter correspond to λ_{ex} = 532 nm

Number of layers	Materials	Thickness (nm)
Air		
24	Si	36.93
23	MoS_2	27.34
2	Si	36.93
1	MoS_2	27.34
Substrate		

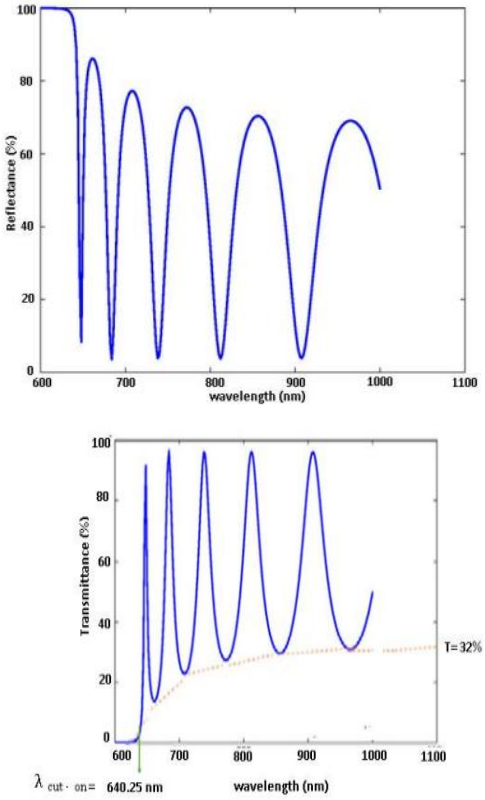


Fig. 3. Reflection and transmittance against λ for λ_{ex} = 633 nm

Table 4. Show layer thickness of 633 nm edge filter

Number of layers	Materials	Thickness (nm)
Air		
24	Si	49.61
23	MoS_2	34.50
2	Si	49.61
1	MoS_2	34.50
Substrate		

Table 5. Show λ_{cut-on} and $\lambda_{cut-off}$ edge filter λ_{ex} 405 nm, 532 nm and 633 nm

S/N	λ_{ex} (nm)	λ_{cut-on} (nm)	$\lambda_{cut-off}$ (nm)
1	405	408.11	700.00
2	532	540.00	800.00
3	633	640.25	1000.00

There are three separate edge filters, each with its own function.

λ_{cut-on} and $\lambda_{cut-off}$

Everything has its own settings. The data in Table 5 was obtained using three distinct filters.

4. CONCLUSION

The modeling, using Octave software and the Raman shift equation, demonstrates that the differences between cutoT and cut off are not significant. The eS values for wavelengths of 405 nm, 532 nm, and 633 nm vary by around 0.2 nm, 1.7 nm, and 1.15 nm, respectively, according to the study. The number discovered for the negative symbol was far higher than previously assumed. When 32% of 633 nm eS, 31.3% of 405 nm, and 31.3% of 532 nm can pass through each filter, the MET number is met.

REFERENCES

1. Butt MA, Fomchenkov SA, Ullah A, Habib M, Ali RZ, Butt A, "Modelling of multilayer dielectric filters based on TiO 2 / SiO 2 and TiO 2 / MiF 2 for fluorescence microscopy imaging M.A. Butt et al." Comput. Opt. 2016;40(5):3–7.
2. Elyutin VV, Butt MA, Khonina SN. "Cold mirror based on High-Low-High refractive index dielectric materials," in 3nd international conference'. Information Technology and Nanotechnology. 2017;1: 5–9.
3. Piegari A, Flory F, Optical thin films and coatings: From materials to applications. United kingdom: Elsevier; 2013.
4. Ng RC, Garcia JC, Greer JR, Fountaine KT, "Polarization-independent, narrow-band, near-ir spectral filters via guided mode resonances in ultrathin a-sianopillar arrays". ACS Photonics; 2019.
5. Nazar A, Ali AH, Jasem NA, "New construction stacks for optimization designs of edge filter new construction stacks for optimization designs of edge filter." 2016;8(3).